Talanta 89 (2012) 27–32

Contents lists available at SciVerse ScienceDirect

Talanta

journal homepage: www.elsevier.com/locate/talanta

# Electrochemiluminescence immunosensor based on graphene–CdS quantum dots–agarose composite for the ultrasensitive detection of alpha fetoprotein

Zhiyong Guo*, Tingting Hao, Jing Duan, Sui Wang, Danyi Wei

*Faculty of Materials Science and Chemical Engineering, Ningbo University, Ningbo, Zhejiang 315211, PR China*

ARTICLE INFO

*Article history:*
Received 23 August 2011
Received in revised form 30 October 2011
Accepted 3 November 2011
Available online 18 November 2011

*Keywords:*
Electrochemiluminescence immunosensor
Alpha fetoprotein
Graphene–CdS QDs–agarose composites
Quantum dots
Graphene
Agarose

ABSTRACT

A novel strategy for the enhancement of electrochemiluminescence (ECL) was developed by combining CdS quantum dots (QDs), graphene (G) and agarose. This enhanced ECL was exploited to develop a label-free ECL immunosensor for the ultrasensitive detection of alpha fetoprotein (AFP). The novel G–CdS QDs–agarose composite was first coated on the glass carbon electrode surface to form a robust film, which exhibited high ECL intensity, good biocompatibility and high stability. After that 3-aminopropyltriethoxysilane (APS), as a binding linker, was conjugated to the G–CdS QDs–agarose composite film on the electrode, the ECL signal was significantly enhanced. The fabrication of ECL immunosensor was successfully completed by immobilizing the AFP-antibody (Ab) onto the electrode through glutaric dialdehyde (GLD). The specific immunoreaction between AFP and antibody resulted in the decrease in ECL intensity and the intensity decreased linearly with the logarithm of AFP concentration in the range of 0.0005–50 pg $mL^{-1}$ with a detection limit of 0.2 fg $mL^{-1}$. The immunosensor exhibits high sensitivity, specificity, stability, reproducibility and good regeneration, thus has the potential to be used in clinical application. Besides, the highly enhanced ECL from the G–CdS QDs–agarose composite film opened new avenues to apply graphene and QDs ECL in analytical systems and ECL biosensors.



## 1. Introduction

Tumor marker is a protein associated with cancer and whose measurement or identification plays an important role in patient diagnosis and clinical research [1]. Alpha fetoprotein (AFP) is considered to be a diagnostic and prognostic tumor marker, implicating the development of human hepatocellular carcinoma (HHC) [2,3]. So the ultrasensitive detection of AFP is worthwhile for early diagnosis of serious hepatitis and evaluating clinical results. The methods currently available for the determination of AFP mainly include enzyme-linked immunosorbent assay (ELISA) [4], electrochemistry [5], fluorescence polarization immunoassay (FPIA) [6] and electrochemiluminescence (ECL) [7–9]. Although great achievement has been obtained in this field, it was still a challenge for the fabrication of novel immunosensors using new materials to achieve more sensitive, faster and more facile detection.

The emergence of nanomaterials provides an excitingly new possibility for advanced development of new analytical tools and instrumentation for bioanalytical applications. Graphene (G), as a new class of one-atom-thick, two-dimensional carbon material with outstanding electronic, optical and mechanical properties [10,11], has been intensively investigated in recent years. Due to its high surface area [12], excellent conductivity [13], unique graphitized basal plane structure and low manufacturing cost [14], both graphene and its composites are considered as ideal electrode materials and has made an impact in the field of electrochemical catalysis, sensing and biosensing [12,15–18]. Semiconductor nanocrystals, known as quantum dots (QDs), were also used for the synthesis of graphene–QDs composites. Research on graphene–QDs composites was mainly focused on their optoelectronic behavior; while their application in immunoassay has been scarcely reported [19].

Electrochemiluminescence (ECL) as a valuable detection method is being applied extensively due to its acknowledged advantages such as versatility, simplified optical setup, very low background signal, and good temporal and spatial control [20]. In the last decade, special ECL behavior of QDs was identified [21–23], and used as ECL reagents in bioanalytical applications [24–26]. However, there exist some limitations associated with the ECL of QDs in bioassays. For instance, the ECL signals of QDs are lower than those of conventional luminescent reagents such as luminol or $Ru(bpy)_3^{2+}$, and QDs themselves are mostly not so biocompatible. Therefore, they have to be surface-modified before they are used in live cell or animal experiments. Up to now, carbon nanotubes (CNTs) [27], poly(diallyldimethylammonium chloride) (PDDA) [25] and gold nanoparticles (AuNPs) [28] were used to

* Corresponding author. Tel.: +86 574 87600798.
*E-mail address:* nbuguo@163.com (Z. Guo).

0039-9140/$ – see front matter © 2011 Elsevier B.V. All rights reserved.
doi:10.1016/j.talanta.2011.11.017

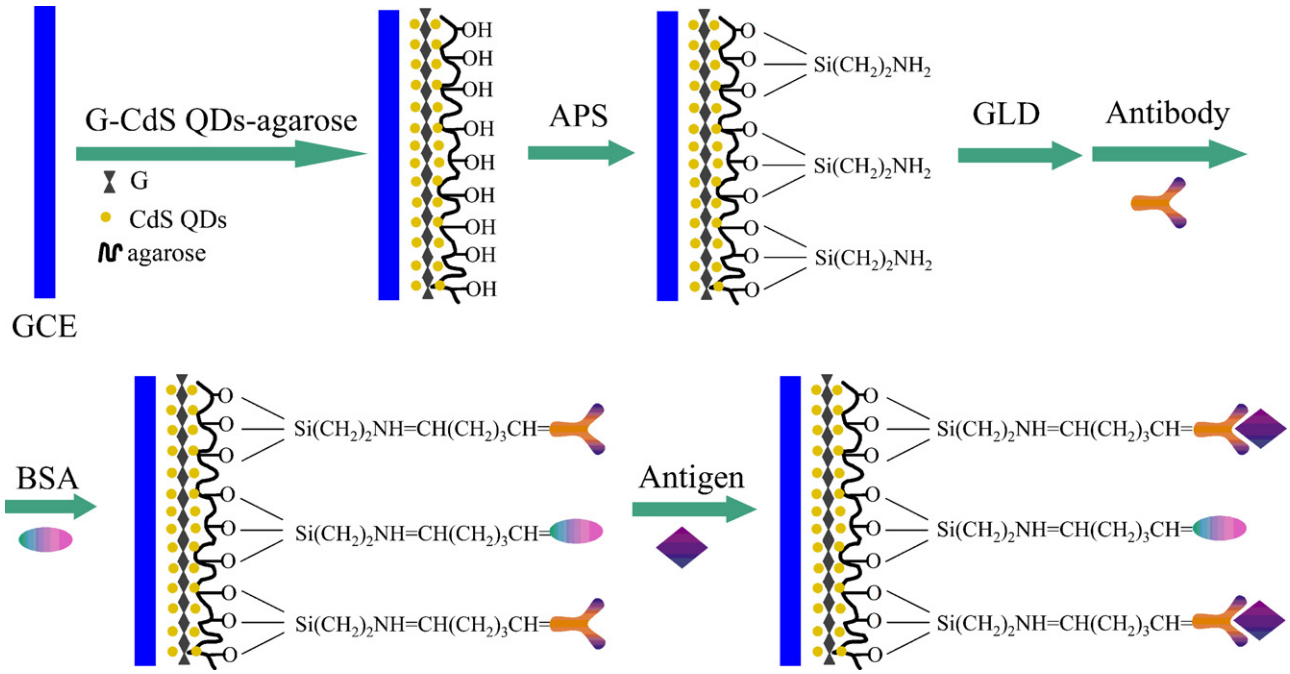


**Fig. 1.** Fabricating steps of the ECL immunosensor.

modify the QDs. Recently, graphene was also used for the synthesis of graphene–QDs composites that enhanced the ECL signal of QDs [19].

Agarose is a polysaccharide with an average molecular weight of 120,000 Da, consisting of 1,3-L-D-galactopyranose and 1,4-linked 3,6-anhydro-k-L-galactose units [29]. Properties of agarose gel matrix such as strong elasticity, high turbidity, aqueous microenvironment and bioaffinity make the agarose an ideal biopolymer to immobilize materials on solid substrates. Its application in direct electrochemistry was reported previously [30,31]. However, to the best of our knowledge, there is no report about its application in immunoassay.

In this work, we developed a novel ECL immunosensor for AFP detection based on G–CdS QDs–agarose composites, which was directly immobilized onto the glass carbon electrode. The detection limit of the developed ECL immunosensor was 0.2 fg $mL^{-1}$. It is close to ten times lower than the lowest one in previous reports [8]. Our method was successfully applied for direct determination of AFP levels in saliva samples. The immunoassays of real samples showed excellent results with high sensitivity and specificity, good reproducibility and long-term stability.

## 2. Materials and methods

### 2.1. Chemicals and solutions

Anti-AFP and AFP were purchased from Biocell Company (Zhengzhou, China) and stored at −20 °C before being used. Graphite powder (8000 mesh, 99.95%) was obtained from Aladdin (Shanghai, China). Bovine serum albumin (BSA, 98–99%) was obtained from Sigma–Aldrich (Steinhem, Germany). Potassium permanganate ($KMnO_4$, 98 wt%), sulfuric acid ($H_2SO_4$, 98 wt%), potassium peroxydisulfate ($K_2S_2O_8$, 99 wt%), phosphorus pentoxide ($P_2O_5$, 99 wt%), hydrogen peroxide ($H_2O_2$, 30 wt%), hydrochloric acid (HCl, 37 wt%), N,N-dimethylformamide (DMF, 98 wt%), sodium hydroxide (NaOH, 96 wt%), cadmium chloride ($CdCl_2$), hydrazine hydrate (80%), thioacetamide, sodium hexametaphosphate, 3-aminopropyl-triethoxysilane (APS), glutaric dialdehyde (GLD) and agarose were obtained from Shanghai Chemical Reagent Co. Ltd. (Shanghai, China). All other reagents were of analytical grade or above and used as received without further purification.

Phosphate buffer solutions (PBS) at the concentration of 0.1 mol $L^{-1}$ with varying pH were prepared by mixing the stock solutions of $NaH_2PO_4$ and $Na_2HPO_4$, and then adjusting the pH with 0.1 mol $L^{-1}$ NaOH and $H_3PO_4$. A 0.1 mol $L^{-1}$ PBS, pH 7.4, containing 0.1 mol $L^{-1}$ $K_2S_2O_8$ and 0.1 mol $L^{-1}$ KCl was used as the electrolyte in ECL analysis. Double distilled water was used throughout the experiment.

### 2.2. Apparatus

A laboratory-built ECL detection system was used as described previously [32]. A conventional three-electrode configuration was employed with bare or modified glass carbon electrode (3 mm diameter) as working electrode, platinum wire as the counter electrode, and an Ag/AgCl (sat. KCl) electrode as the reference electrode. Electrochemical impedance spectroscopy (EIS) was carried out with a CHI 660D electrochemical workstation (Shanghai CH Instrument Co., Shanghai, China), using the same three-electrode system similar to the ECL detection. The spectral width of the photomultiplier tube (PMT) was 200–800 nm and the voltage was 600–800 V in the detection process. Photoluminescence (PL) spectra were acquired on a Hitachi F-4600 spectrofluorometer (Tokyo, Japan). UV–vis absorption spectra were recorded with a Persee General TU-1901 spectrophotometer (Beijing, China). Hitachi SU-70 scanning electron microscope (SEM, Tokyo, Japan) was used to characterize the sensor.

### 2.3. Synthesis of graphene

Graphite oxide (GO) was synthesized from graphite powder using a method as presented by Kovtyukhova et al. [33]. Exfoliation was carried out by dispersing the GO for 2 h using sonication, and the small amount of unexfoliated GO was removed by centrifugation at 3000 rpm. The concentration of GO was determined by UV–vis spectroscopy and further determined by a gravimetric method. Graphene (G) solution was prepared according to Li et al. [34] with a minor modification. Briefly, 9.6 μL of hydrazine solution

(80%) and 105 μL of ammonia (35%) was added into the GO solution obtained. The weight ratio of hydrazine to GO was about 7:10. After being vigorously shaken for a few minutes, the vial was put in an oil bath (~98 °C) for 1 h.

### 2.4. Preparation of G–CdS QDs–agarose composite

CdS QDs were prepared as described previously [35]. Briefly, 10 mL of 0.01 mol $L^{-1}$ cadmium chloride was mixed with 10 mL of 0.01 mol $L^{-1}$ thioacetamide and 1 mL of 0.1 mol $L^{-1}$ sodium hexametaphosphate; and the pH of the solution was adjusted to 10. After reacted for about 30 min, the solution became yellow indicating the formation of CdS QDs. Then, the solution was centrifuged at 12,000 rpm that concentrated the CdS QDs about 100 times.

Agarose hydrogel solution, 4 mg $mL^{-1}$, was prepared according to our previous report [30]. Briefly, 0.2 g agarose was dissolved in 50 mL boiling water, and then the solution obtained was cooled for use.

The G solution and agarose hydrogel solution were mixed in the volume ratio of 1:1 under vortex shaking for 30 min. The G–CdS QDs–agarose composite solution was obtained by mixing the condensed CdS QDs solution and the G–agarose composite solution in the volume ratio of 1:1 under vortex shaking for 30 min.

### 2.5. Preparation of the ECL immunosensor

A 3 mm diameter glass carbon electrode was polished successively with 1.0, 0.3 and 0.05 μm α-$Al_2O_3$ powder on fine abrasive paper; subjected to ultrasonic treatment in water; rinsed thoroughly with water and allowed to dry at room temperature. Then 10 μL of G–CdS QDs–agarose composite solution was dropped on the electrode and dried in the air, followed by immersing the electrode in 2% APS solution for 1.5 h to introduce the amine functional groups. Then, the electrode was rinsed with water and dipped in 2.5% GLD solution at room temperature for 15 min and then in 0.5 mg $mL^{-1}$ antibody solution at 4 °C for 18–24 h. Finally, it was rinsed with pH 7.4 PBS and incubated in 20 μL of 2 (wt%) BSA at 37 °C for 1 h to block nonspecific binding sites. After being rinsed with pH 7.4 PBS again, the electrode was used as an ECL immunosensor and incubated in 40 μL of AFP (Ag) samples at 37 °C for 50 min.

Fig. 1 outlines the fabrication of the ECL immunosensor, which included the formation of the G–CdS QDs–agarose composite film on the glass carbon electrode (GCE), the linkage of APS with the film, the covalent conjugation of GLD with APS, the immobilization of antibody on the electrode by GLD, and the specific immunoreaction.

### 2.6. ECL detection

The modified electrodes as described in Section 2.5 were in contact with 0.1 mol $L^{-1}$ PBS at pH 7.4 containing 0.1 mol $L^{-1}$ $K_2S_2O_8$ and 0.1 mol $L^{-1}$ KCl, and scanned from 0 V to −1.6 V. ECL signals produced in response to the AFP concentrations were measured.

## 3. Results and discussion

### 3.1. Characterization of G and CdS QDs

Graphene, which was reduced by hydrazine solution, was negatively charged [36]. When G and agarose were mixed by vortex shaking, agarose molecules were adsorbed on the surface of G by electrostatic interaction, which would resist the aggregation of G effectively. As a result, a homogeneous black solution was obtained.

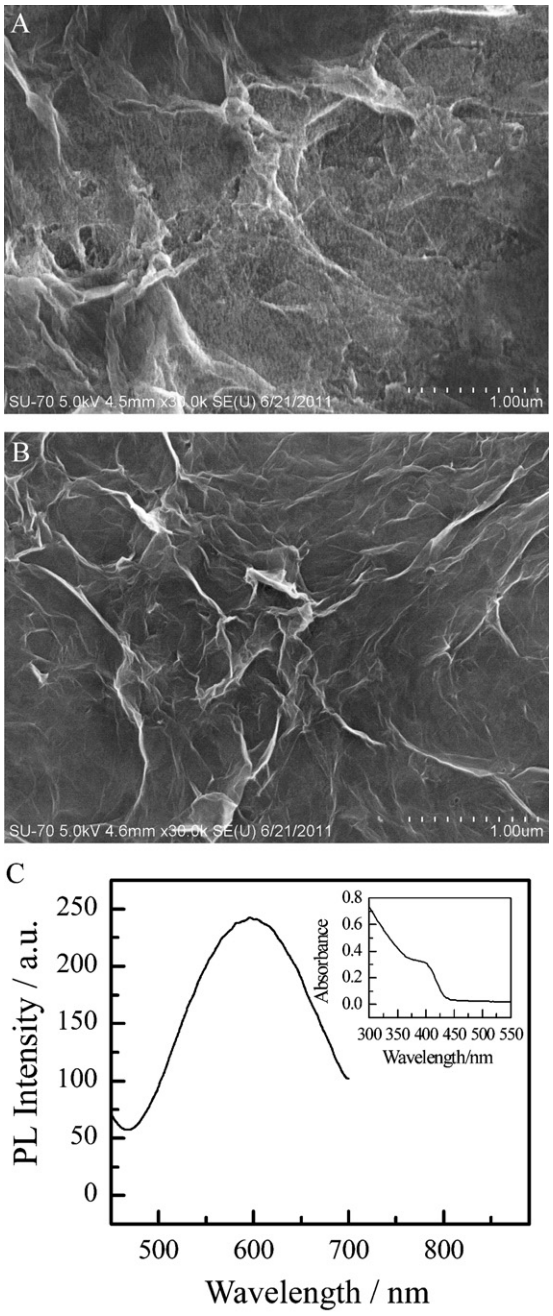


**Fig. 2.** Representative SEM images of (A) graphene (G) and (B) G–agarose, and (C) photoluminescence and absorption (inset) spectra of the CdS QDs in aqueous solution. Excitation wavelength: 370 nm.

As shown in Fig. 2A, large flakes of G were dispersed. There were some monolayer G with slightly scrolled edges and some G flakes folded together. While in Fig. 2B, the more homogeneous structure could be observed for the G–agarose, and the surface was much rougher which was favorable for the construction of the ECL immunosensor [37].

The PL and UV–vis absorption spectra (inset) of the CdS QDs were shown in Fig. 2C. The PL emission peak was at 616 nm ($\lambda_{ex}$ = 370 nm) and the maximum absorption wavelength was at 400 nm, indicating the consequence of quantum confinement [38,39]. The size of the CdS QDs, estimated from the absorption peak in UV–vis spectra and the empirical equations [40], was about 3.0 nm.

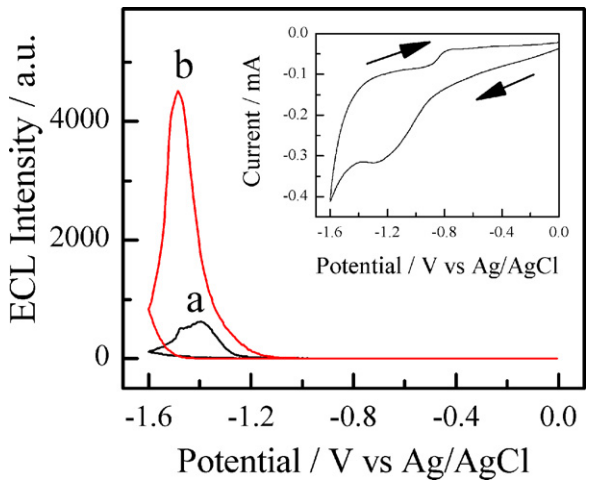


**Fig. 3.** ECL–potential curves of (a) the CdS QDs modified GC electrode and (b) the G–CdS QDs–agarose composite film modified GC electrode in 0.1 mol $L^{-1}$ PBS at pH 7.4 containing 0.1 mol $L^{-1}$ KCl and 0.1 mol $L^{-1}$ $K_2S_2O_8$. The voltage of the photomultiplier tube was set at 700 V. Inset: cyclic voltammogram of the G–CdS QDs–agarose composite modified GC electrode. Scan rate: 50 mV $s^{-1}$.

### 3.2. Electrochemical and ECL behaviors of the G–CdS QDs–agarose composite film

Fig. 3 shows the ECL intensity–potential curves of the pure CdS QDs film (curve a) and the G–CdS QDs–agarose composite film (curve b) modified electrode, respectively. The quantities of the CdS QDs were equal in both films. The ECL intensity from the G–CdS QDs–agarose composite film was about 7 times higher than the ECL observed from the pure CdS QDs film. The results indicated that high porous structure, large surface area, and good conductivity of G–CdS QDs–agarose composite film facilitated the ECL reaction. Thus, the G–CdS QDs–agarose composite film was very promising for the construction of the ECL biosensor.

The inset showed the cyclic voltammogram of G–CdS QDs–agarose composite film on the electrode. One cathodic peak at about −1.2 V was observed, resulting from the reaction of CdS QDs with $S_2O_8^{2-}$. Herein, the CdS QDs were reduced to $CdS^{\bullet-}$, while the coreactant $S_2O_8^{2-}$ was reduced to $SO_4^{\bullet-}$. Then $SO_4^{\bullet-}$ reacted with $CdS^{\bullet-}$ through electron transfer that produced the excited state ($CdS^*$) to emit light [24].

### 3.3. Characterization of the ECL immunosensor

#### 3.3.1. SEM images

Fig. 4A–C displays the typical SEM images of G–CdS QDs–agarose, G–CdS QDs–agarose/APS and G–CdS QDs–agarose/APS/GLD/Ab assembled on the electrode surface, respectively. As seen in Fig. 4A, the CdS QDs were distributed uniformly in the G–agarose, and a homogeneous film was formed on the electrode. When APS was conjugated to the nanocomposites, the well-dispersed film spread over the electrode more uniformly (Fig. 4B). After Ab was immobilized onto the electrode, the composite film became much rougher (Fig. 4C) and the structure of film was completely changed, confirming the completion of immunosensor fabrication.

#### 3.3.2. Electrochemiluminescence behavior

ECL signals at each immobilization steps were recorded to monitor the fabrication process of the ECL immunosensor. As shown in Fig. 4D, when APS was conjugated to the G–CdS QDs–agarose composite film (curve a), the ECL intensity was greatly enhanced (curve b), due to the amine groups of APS that facilitated the radical generation and electron-transfer processes during the ECL reaction [37]. When antibody (Ab) was immobilized onto the electrode (curve c), BSA was used to block the nonspecific binding sites (curve d) and the immunoreaction occurred (curve e); consequently the ECL intensity decreased gradually due to the antigen–antibody complex and the BSA protein on the electrode. They acted as the inert electron and mass-transfer blocking layer, hindering the diffusion of ECL reagents toward the electrode surface significantly that led to the ultimate decrease of ECL signal.

#### 3.3.3. EIS behavior

EIS is an effective method for probing the features of surface modified electrodes. Fig. 4E is the typical Nyquist plot ($-Z''$ vs. $Z'$) for the electrode at different stages. The diameter of semicircle at higher frequencies corresponds to the electron transfer resistance $R_{et}$. It could be found that G–CdS QDs–agarose modified electrode (curve b) showed a lower $R_{et}$ than pure CdS QDs modified one (curve a), implying that G–CdS QDs–agarose possessed excellent electrical conductivity and was able to accelerate the electron transfer. Subsequently, APS was covalently conjugated to the composite film (curve c), followed by GLD (curve d) resulting in successive increase in $R_{et}$. In the final step, the immobilization of antibody generated an insulating protein layer on the assembled surface and prevented the probe redox pair $[Fe(CN)_6]^{3-/4-}$ from nearing the electrode surface resulting in further increase of $R_{et}$ (curve e).

### 3.4. Optimization of experimental conditions

The ECL performance of the immunosensor mainly depended on the ratio of CdS QDs, G and agarose. The results revealed that the optimal volume ratio of the condensed CdS QDs solution, G solution (0.5 mg $mL^{-1}$) and agarose hydrogel solution (4 mg $mL^{-1}$) was 2:1:1, respectively.

The effects of incubation temperature, incubation time and pH value on the ECL intensity of the immunosensor were also investigated. The incubation temperature of 37 °C and the incubation time of 50 min were selected for the ECL immunosensor. The optimal pH value for the biological systems was 7.4, and the ECL detection was performed in pH 7.4 PBS containing 0.1 mol $L^{-1}$ $K_2S_2O_8$ and 0.1 mol $L^{-1}$ KCl.

### 3.5. Detection of AFP (Ag)

Fig. 5A shows the ECL emission of the immunosensor under consecutive potential scans from 0 to −1.6 V for 15 cycles. The ECL signals were high and stable, suggesting that the sensor was suitable for ECL detection.

Fig. 5B shows the ECL responses of the immunosensor before (a) and after (b–g) reacting with different concentrations of AFP (Ag). The ECL peak intensity in the presence of Ag was lower than that in the absence of Ag (a), and decreased gradually with increasing concentrations of Ag (b → g). The reasons behind this behavior were (1) the immunocomplex increased the steric hindrance, slowed down the electron transfer speed in ECL reaction and thus decreased the ECL intensity and (2) the transfer of coreactant $K_2S_2O_8$ to the surface of the G–CdS QDs–agarose composite film modified electrode was inhibited.

The standard calibration curve for AFP detection was shown in Fig. 5B (inset). The ECL intensity ($y$) decreased with the logarithm of the AFP concentrations ($x$) in the range from 0.0005 to 50 pg $mL^{-1}$. The regression equation was $y = 2674.22 - 828.03 \log x$ (pg $mL^{-1}$), with a correlation coefficient $r$ of 0.9948. The limit of detection (LOD) was about 0.0002 pg $mL^{-1}$ (0.2 fg $mL^{-1}$) and the limit of quantification (LOQ) was 0.0005 pg $mL^{-1}$ (0.5 fg $mL^{-1}$), indicating

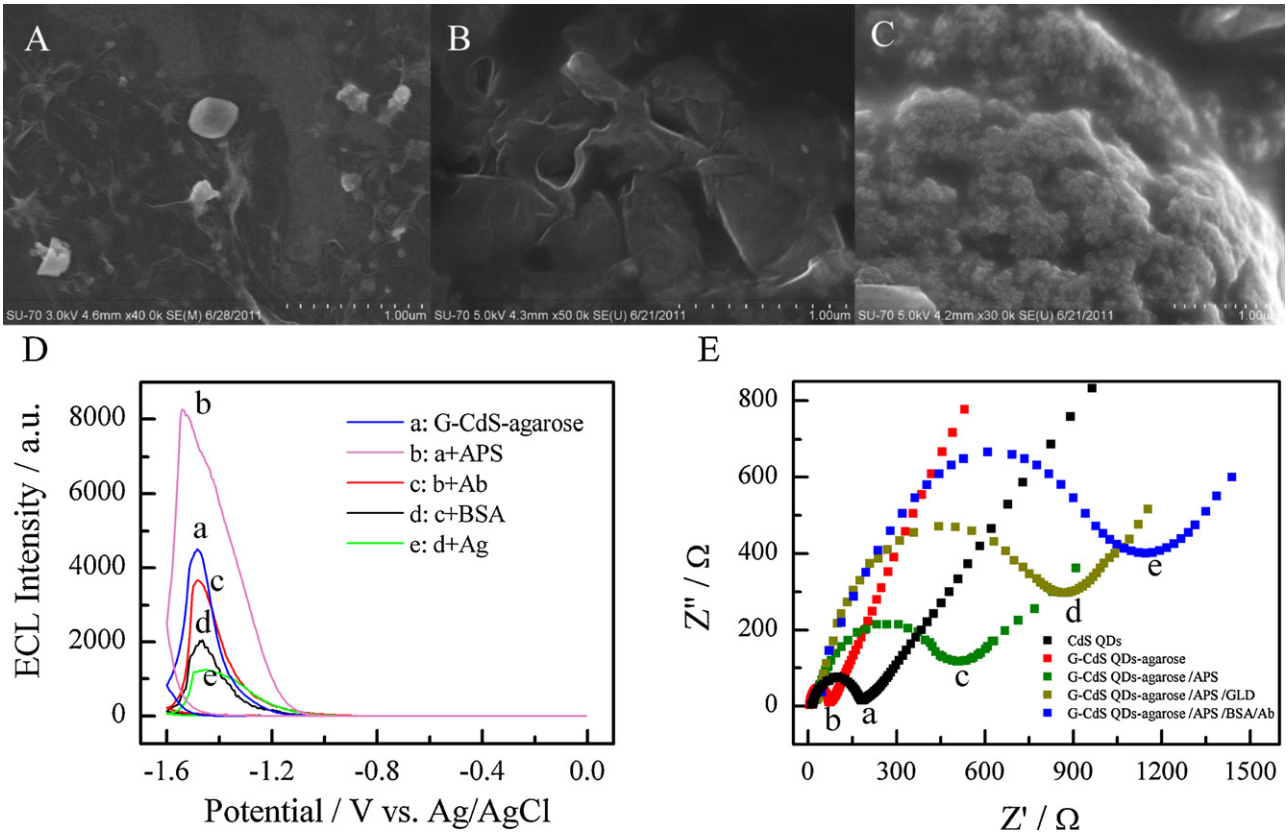


**Fig. 4.** Representative SEM images of (A) G–CdS QDs–agarose, (B) (A) + APS, (C) (B) + Ab; (D) ECL–potential curves of (a) G–CdS QDs, (b) (a) + APS, (c) (b) + Ab, (d) (c) + BSA, and (e) (d) + Ag modified GC electrodes in 0.1 mol $L^{-1}$ PBS at pH 7.4 containing 0.1 mol $L^{-1}$ KCl and 0.1 mol $L^{-1}$ $K_2S_2O_8$. The voltage of the photomultiplier tube was set at 700 V. Scan rate: 50 mV $s^{-1}$; (E) electrochemical impedance spectroscopy (EIS) of (a) CdS QDs, (b) G–CdS QDs–agarose, (c) (b) + APS, (d) (c) + GLD + GLD, and (e) G–CdS QDs–agarose/APS/BSA/Ab modified GC electrodes in 10 mmol $L^{-1}$ PBS (2.5 mmol $L^{-1}$ $Fe(CN)_6^{4-/3-}$ + 0.1 mol $L^{-1}$ mol/L KCl, pH 7.4). The frequency range was between 0.01 and 100,000 Hz with a signal amplitude of 5 mV.

that this method is very sensitive for the determination of AFP. Literature search clearly indicates that the sensitivity of this method for the determination of AFP was about ten times lower than the lowest one previously reported [8,41–43]. In addition, the wide linear concentration range is very favorable for the clinical applications. If serum AFP levels were higher beyond this linear range, samples could be detected by an appropriate dilution with pH 7.4 PBS.

### 3.6. Specificity, stability, reproducibility, and regeneration of the immunosensor

In order to illustrate the specificity of the immunosensor proposed, 0.05 pg $mL^{-1}$ AFP, 5 ng $mL^{-1}$ carbohydrate antigen 19-9 (CA19-9), 5 ng $mL^{-1}$ carcinoembryonic antigen (CEA), 5 ng $mL^{-1}$ human chorionic gonadotropin (HCG) and 5 ng $mL^{-1}$ Hepatitis B surface antigen (HBsAg) were mixed, and the ECL response of the mixture was determined. Compared with the ECL response of the immunosensor in 0.05 pg $mL^{-1}$ pure AFP, no significant difference (R.S.D. = 6.3%) was observed, indicating that the CA19-9, CEA, HCG and HBsAg could not bring any observable interference. Therefore, the immunosensor developed has excellent specificity for the determination of AFP.

**Table 1**
Recovery tests for AFP in spiked human serum samples.

| Sample | Original (ng $mL^{-1}$) | Added (ng $mL^{-1}$) | Found (ng $mL^{-1}$) | Recovery (%) |
|---|---|---|---|---|
| Serum 1 | 12.8 | 10 | 21.9 | 91 |
| Serum 2 | 5.6 | 10 | 16.2 | 106 |
| Serum 3 | 9.2 | 10 | 19.6 | 104 |
| Serum 4 | 3.4 | 10 | 13.7 | 103 |
| Saliva 1 | 0.62 | 1.0 | 1.57 | 95 |
| Saliva 2 | 0.26 | 1.0 | 1.35 | 109 |
| Saliva 3 | 1.59 | 1.0 | 2.48 | 89 |
| Saliva 4 | 0.083 | 0.1 | 0.175 | 92 |

The signal of the ECL immunosensor remained about 97.3% of the initial value after the immunosensor was stored in pH 7.4 PBS at 4 °C for 30 days, demonstrating that the immunosensor had a good stability. The reasons could be ascribed to the agarose hydrogel, which is one of the best gels for constructing bioreactors, due to its abilities in providing a well-defined microenvironment to retain the activity of the immobilized antibody and facilitate the electron exchange.

The reproducibility of the immunosensor was evaluated by determining 0.05 pg $mL^{-1}$ AFP with five immunosensors prepared at the same electrode. An average recovery of 94.8% and a relative standard deviation of 6.9% were obtained from five measurements, indicating that the fabrication protocol was reproducible.

Regeneration of the immunosensor is one of the most important problems in immunoassay. Therefore to evaluate the regeneration property, the immunosensor was regenerated by treating the modified electrodes with 0.2 mol $L^{-1}$ glycine–hydrochloric acid (Gly–HCl) buffer solution (pH = 2.8) for 8 min to break the antibody–antigen linkage. One sample was determined for ten times on the same electrode whenever the immunosensor was regenerated. An average recovery of 93.5% and an intra-assay relative standard deviation of 8.6% were obtained at the AFP concentration of 0.05 pg $mL^{-1}$. The results demonstrated that the immunosensor could be regenerated and used for at least ten times.

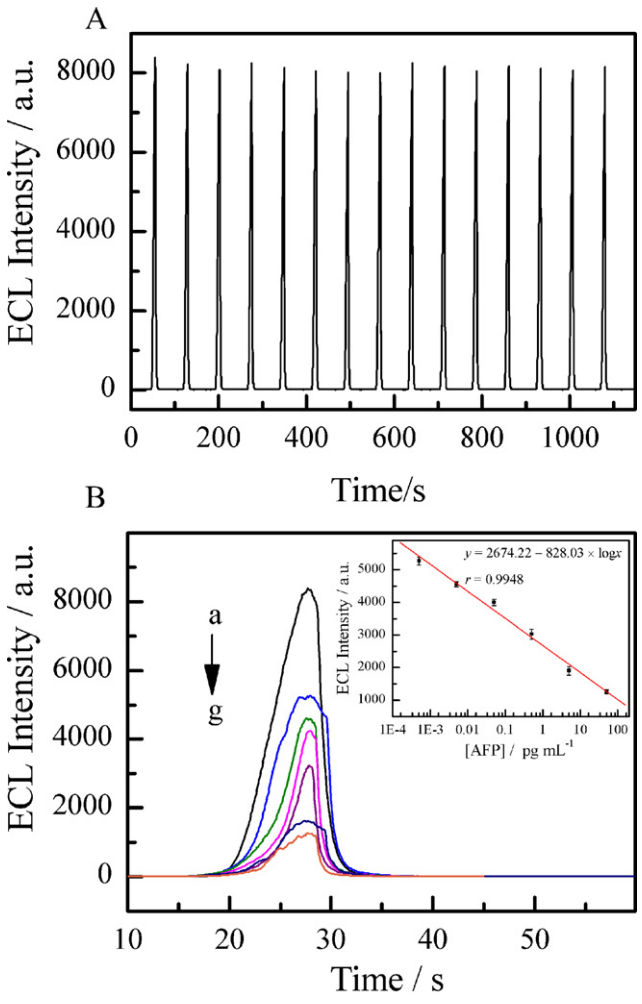


**Fig. 5.** (A) ECL emission from the immunosensor in pH 7.4 PBS containing 0.1 mol $L^{-1}$ KCl and 0.1 mol $L^{-1}$ $K_2S_2O_8$ under continuous cyclic voltammetry for 15 cycles. Scan rate: 50 mV $s^{-1}$. The voltage of the PMT was set at 800 V. (B) ECL profiles of the immunosensor in the absence (a) and presence (b–g) of different concentrations of Ag in pH 7.4 PBS containing 0.1 mol $L^{-1}$ KCl and 0.1 mol $L^{-1}$ $K_2S_2O_8$. Ag concentration (pg $mL^{-1}$): (a) 0, (b) 0.0005, (c) 0.005, (d) 0.05, (e) 0.5, (f) 5, and (g) 50. The voltage of the PMT was set at 800 V. The inset: calibration curve for Ag determination. Scan rate: 50 mV $s^{-1}$.

### 3.7. Application of the immunosensor in AFP levels

The feasibility of the developed ECL immunoassay system for clinical applications was investigated by analyzing several clinical samples. The serum and saliva samples were diluted to suitable concentrations with pH 7.4 PBS and specific quantities of AFP were added. The results showed satisfactory recoveries in the range of 89–109% (Table 1), indicating that the developed ECL immunosensor could be used in clinic applications for the ultrasensitive determination of AFP in human serum and saliva.

## 4. Conclusions

In the present work, a novel label-free ECL immunosensor for the rapid, ultrasensitive detection of AFP was developed. The excellent conductivity, extraordinary electron transport properties and large specific surface area of the G–CdS QDs–agarose composite film resulted in high ECL intensity and excellent film-forming ability that made this composite material a promising candidate to be developed as an ECL immunosensor. The developed immunosensor showed an extremely sensitive response to AFP with a detection limit of 0.2 fg $mL^{-1}$, which was about ten times lower than the lowest one reported before [8]. Besides, specificity, stability, reproducibility, and regeneration of the immunosensor were all satisfactory. Moreover, the potentially enhanced ECL from the G–CdS QDs–agarose composite film opened a new avenue to apply graphene and QDs ECL in other analytical systems and ECL biosensors.

## Acknowledgements

Financial supports from National Natural Science Foundation of China (No. 81072336), 973 Program (2010CB635116), Science and Technology Department of Zhejiang Province of China (2011R405051), Ningbo Science and Technology Bureau (2010A610030, 2011C50037), Fund for Outstanding Young Teachers in Higher Education Institutions of Zhejiang Province and Ningbo University (xk111049) are gratefully acknowledged. This work was also sponsored by K.C. Wong Magna Fund in Ningbo University.

## References

[1] M. Miyake, K. Sugano, H. Sugino, K. Imai, E. Matsumoto, K. Maeda, S. Fukuzono, Y. Hirao, Cancer Sci. 101 (2010) 250.
[2] C.J.P. Smith, P.C. Kelleher, BBA-Rev. Cancer 605 (1980) 1.
[3] H. Yokoo, T. Kondo, K. Fujii, T. Yamada, S. Todo, S. Hirohashi, Hepatology 40 (2004) 609.
[4] S. Sun, R.T.P. Poon, N.P. Lee, C. Yeung, K.L. Chan, I.O.L. Ng, P.J.R. Day, J.M. Luk, J. Proteome Res. 9 (2010) 1923.
[5] C. Ding, F. Zhao, R. Ren, J.M. Lin, Talanta 78 (2009) 1148.
[6] J. Tian, R. Liu, Y. Zhao, Y. Peng, X. Hong, Q. Xu, S. Zhao, Nanotechnology 21 (2010) 305101.
[7] J. Qian, Z. Zhou, X. Cao, S. Liu, Anal. Chim. Acta 665 (2010) 32.
[8] H. Wang, D. Sun, Z. Tan, W. Gong, L. Wang, Colloids Surf. B 84 (2011) 515.
[9] S. Yuan, R. Yuan, Y. Chai, L. Mao, X. Yang, Y. Yuan, H. Niu, Talanta 82 (2010) 1468.
[10] P. Avouris, Z. Chen, V. Perebeinos, Nat. Nanotechnol. 2 (2007) 605.
[11] K. Novoselov, A. Geim, S. Morozov, D. Jiang, Y. Zhang, S. Dubonos, I. Grigorieva, A. Firsov, Science 306 (2004) 666.
[12] W.R. Algar, A.J. Tavares, U.J. Krull, Anal. Chim. Acta 673 (2010) 1.
[13] A.K. Geim, K.S. Novoselov, Nat. Mater. 6 (2007) 183.
[14] H.C. Schniepp, J.L. Li, M.J. McAllister, H. Sai, M. Herrera-Alonso, D.H. Adamson, R.K. Prud'homme, R. Car, D.A. Saville, I.A. Aksay, J. Phys. Chem. B 110 (2006) 8535.
[15] L.Z. Hu, G.B. Xu, Chem. Soc. Rev. 39 (2010) 3275.
[16] J. Li, S.J. Guo, Y.M. Zhai, E.K. Wang, Electrochem. Commun. 11 (2009) 1085.
[17] L. Tang, Y. Wang, Y. Li, H. Feng, J. Lu, J. Li, Adv. Funct. Mater. 19 (2009) 2782.
[18] D. Chen, L. Tang, J. Li, Chem. Soc. Rev. 39 (2010) 3157.
[19] L.L. Li, K.P. Liu, G.H. Yang, C.M. Wang, J.R. Zhang, J.J. Zhu, Adv. Funct. Mater. 21 (2011) 869.
[20] M.M. Richter, Chem. Rev. 104 (2004) 3003.
[21] N. Myung, Y. Bae, A.J. Bard, Nano Lett. 3 (2003) 1053.
[22] Z. Ding, B.M. Quinn, S.K. Haram, L.E. Pell, B.A. Korgel, A.J. Bard, Science 296 (2002) 1293.
[23] N. Myung, Z. Ding, A.J. Bard, Nano Letters 2 (2002) 1315.
[24] G. Jie, P. Liu, L. Wang, S. Zhang, Electrochem. Commun. 12 (2010) 22.
[25] G. Jie, L. Li, C. Chen, J. Xuan, J.J. Zhu, Biosens. Bioelectron. 24 (2009) 3352.
[26] W. Tu, Y. Dong, J. Lei, H. Ju, Anal. Chem. 82 (2010) 8711.
[27] J. Zhang, J. Lei, C. Xu, L. Ding, H. Ju, Anal. Chem. 82 (2010) 1117.
[28] G. Jie, P. Liu, S. Zhang, Chem. Commun. 46 (2010) 1323.
[29] P. Aymard, D.R. Martin, K. Plucknett, T.J. Foster, A.H. Clark, I.T. Norton, Biopolymers 59 (2001) 131.
[30] Z. Guo, H. Zhang, P. Gai, J. Duan, Russ. J. Electrochem. 47 (2011) 175.
[31] H.H. Liu, Z.Q. Tian, Z.X. Lu, Z.L. Zhang, M. Zhang, D.W. Pang, Biosens. Bioelectron. 20 (2004) 294.
[32] Z. Guo, P. Gai, Anal. Chim. Acta 688 (2011) 197.
[33] N.I. Kovtyukhova, P.J. Ollivier, B.R. Martin, T.E. Mallouk, S.A. Chizhik, E.V. Buzaneva, A.D. Gorchinskiy, Chem. Mater. 11 (1999) 771.
[34] D. Li, M.B. Müller, S. Gilje, R.B. Kaner, G.G. Wallace, Nat. Nanotechnol. 3 (2008) 101.
[35] H. Wang, X. Zhang, Z. Tan, W. Yao, L. Wang, Electrochem. Commun. 10 (2008) 170.
[36] Y. Chen, Y. Li, D. Sun, D. Tian, J. Zhang, J.J. Zhu, J. Mater. Chem. 21 (2011) 7604.
[37] G. Jie, J. Zhang, D. Wang, C. Cheng, H.Y. Chen, J.J. Zhu, Anal. Chem. 80 (2008) 4033.
[38] A.P. Alivisatos, J. Phys. Chem. 100 (1996) 13226.
[39] A.P. Alivisatos, Science 271 (1996) 933.
[40] W.W. Yu, L.H. Qu, Z.H. Guo, X.G. Peng, Chem. Mater. 15 (2003) 2854.
[41] X.Y. Yang, Y.S. Guo, S. Bi, S.S. Zhang, Biosens. Bioelectron. 24 (2009) 2707.
[42] Z.J. Yang, H. Liu, C. Zong, F. Yan, H.X. Ju, Anal. Chem. 81 (2009) 5484.
[43] X. Wang, Q.Y. Zhang, Z.J. Li, X.T. Ying, J.M. Lin, Clin. Chim. Acta 393 (2008) 90.